



Title	Preparation of superparamagnetic magnetite nanoparticles by reverse precipitation method: Contribution of sonochemically generated oxidants.
Author(s)	Mizukoshi, Yoshiteru; Shuto, Tatsuya; Masahashi, Naoya; Tanabe, Shuji
Citation	Ultrasonics Sonochemistry, 16(4), pp.525-531; 2009
Issue Date	2009-04
URL	<a href="http://hdl.handle.net/10069/20929">http://hdl.handle.net/10069/20929</a>
Right	Copyright © 2009 Elsevier B.V. All rights reserved.

This document is downloaded at: 2020-10-26T16:27:08Z

Elsevier Editorial System(tm) for Ultrasonics Sonochemistry  
Manuscript Draft

Manuscript Number: ULTSON-D-08-00264R1

Title: Preparation of superparamagnetic magnetite nanoparticles by reverse precipitation method:  
Contribution of sonochemically generated oxidants

Article Type: Full Length Article

Keywords: Magnetic nanoparticle; Magnetite; Sonochemical oxidation

Corresponding Author: Dr. Yoshiteru Mizukoshi,

Corresponding Author's Institution: Tohoku Univ.

First Author: Yoshiteru Mizukoshi

Order of Authors: Yoshiteru Mizukoshi; Tatsuya Shuto; Naoya Masahashi; Shuji Tanabe

Abstract: Magnetic iron oxide nanoparticles were successfully prepared by a novel reverse precipitation method with the irradiation of ultrasound. TEM, XRD and SQUID analyses showed that the formed particles were magnetite ( $\text{Fe}_3\text{O}_4$ ) with about 10 nm in their diameter. The magnetite nanoparticles exhibited superparamagnetism above 200 K, and the saturation magnetization was 32.8 emu/g at 300 K. The sizes and size distributions could be controlled by the feeding conditions of  $\text{FeSO}_4 \cdot 7\text{H}_2\text{O}$  aqueous solution, and slower feeding rate and lower concentration lead to smaller and more uniform magnetite nanoparticles. The mechanisms of sonochemical oxidation were also discussed. The analyses of sonochemically produced oxidants in the presence of various gases suggested that besides sonochemically formed hydrogen peroxide, nitrite and nitrate ions contributed to Fe(II) ion oxidation.

Preparation of superparamagnetic magnetite nanoparticles by reverse precipitation  
method: Contribution of sonochemically generated oxidants

Corresponding Author :

Dr. Yoshiteru Mizukoshi

Osaka Center for Industrial Materials Research, Institute for Materials Research,  
Tohoku University

Address: 1-2 Gakuen-cho, Naka-ku, Sakai, Osaka 599-8531, Japan

Telephone: +81-(0)72-254-6372

Fax: +81-(0)72-254-6375

e-mail: [mizukosi@imr.tohoku.ac.jp](mailto:mizukosi@imr.tohoku.ac.jp)

Preparation of superparamagnetic magnetite nanoparticles by reverse precipitation method: Contribution of sonochemically generated oxidants

Yoshiteru Mizukoshi<sup>1</sup>, Tatsuya Shuto<sup>2</sup>, Naoya Masahashi<sup>1</sup>, Shuji Tanabe<sup>2</sup>

<sup>1</sup>Institute for Materials Research, Tohoku University, Japan

<sup>2</sup>Graduate School of Science and Technology, Nagasaki University, Japan

Abstract

Magnetic iron oxide nanoparticles were successfully prepared by a novel reverse precipitation method with the irradiation of ultrasound. TEM, XRD and SQUID analyses showed that the formed particles were magnetite ( $\text{Fe}_3\text{O}_4$ ) with about 10 nm in their diameter. The magnetite nanoparticles exhibited superparamagnetism above 200 K, and the saturation magnetization was 32.8 emu/g at 300 K. The sizes and size distributions could be controlled by the feeding conditions of  $\text{FeSO}_4 \cdot 7\text{H}_2\text{O}$  aqueous solution, and slower feeding rate and lower concentration lead to smaller and more uniform magnetite nanoparticles. The mechanisms of sonochemical oxidation were also discussed. The analyses of sonochemically produced oxidants in the presence of various gases suggested that besides sonochemically formed hydrogen peroxide, nitrite and nitrate ions contributed to Fe(II) ion oxidation.

PACS code      Magnetic materials, 75.50

Keywords        Magnetic nanoparticle; Magnetite; Sonochemical oxidation

## 1. Introduction

Magnetic substances, which have been utilized for motors, power distribution systems etc., are ones of the most familiar functional materials, and are indispensable to daily life [1]. Among the magnetic substances, magnetic nanoparticles have been extensively studied for the applications for magnetic fluids [2, 3], magnetic separable catalysts [4, 5], data storage media [6], and environmental remediation [7, 8]. Especially in the field of biotechnologies and bio-engineering, the magnetic nanoparticles are promising for applications such as separations of biochemical species [9, 10], cell separation [11], drug deliveries [12], biomedical imaging [13], hyperthermia [14].

Small sizes (<100 nm), uniform morphologies, soft magnetisms and high dispersity are required for the practical uses of magnetic nanoparticles in biotechnology because the magnetic properties greatly depend on the morphologies of the nanoparticles and their residual magnetism induces aggregation among the particles. When the particle size is adequately small, the each particle is a single magnetic domain and exhibits superparamagnetic property above the blocking temperature [15, 16]. Superparamagnetic nanoparticles quickly respond to the applied external magnetic field, and their remanence and coercivity are negligible. Accordingly, when superparamagnetic nanoparticles are used in the field of bio, undesirable particle agglomerations originated from the residual magnetism can be avoided.

Iron oxide, i.e. maghemite ( $\gamma\text{-Fe}_2\text{O}_3$ ) and magnetite ( $\text{Fe}_3\text{O}_4$ ) nanoparticles are typical magnetic nanoparticles and are generally prepared by precipitation method, wherein the reaction time is relatively short, water is used as solvent and it is easy to gain high yields by scale-up. On the negative side of this method, it is difficult to control the size, size distribution and shape of the formed oxide particles [15].

We reported the preparation of magnetite nanoparticles by sonochemical oxidation of aqueous  $\text{Fe}(\text{OH})_2$  suspension obtained by adding aqueous NaOH solution to aqueous  $\text{FeSO}_4 \cdot 7\text{H}_2\text{O}$  solution (hereafter, this protocol is referred as normal precipitation method; NP method), however, the obtained magnetite nanoparticles were in relatively large (ca. 40 nm) and irregular in morphology (Fig.1) [17].

In NP method wherein an alkaline aqueous solution is added to an aqueous solution containing metal salt, the pH value of solution changes rapidly and locally. Accordingly, it is difficult to synthesize smaller and more uniform-shaped products which are desirable for the practical uses. To keep homogeneity of the reaction system during the formation process of the metal hydroxides, Teraoka et. al. reported reverse homogeneous precipitation(RHP) method [18]. In RHP method, an acidic solution of metal salt is added dropwise to a basic solution of alkaline, in contrast to NP method.

The objective of this study is to develop a new preparation method of magnetite nanoparticles by RHP method with the assistance of ultrasound. It is expected that smaller and more uniform-shaped nanoparticles can be formed by uses of ultrasound due to the effective agitation and in situ formation of active chemical species formed via cavitation collapse [19].

## **2. Experimental**

All chemicals were purchased from Wako Pure Chemicals and used as received. An aqueous solution of  $\text{FeSO}_4 \cdot 7\text{H}_2\text{O}$  was fed into an aqueous solution containing NaOH and polyethylene glycol monostearate (PEG-MS) added as a protective agent. Polyethyleneglycol is one of the most popular materials to modify particles surfaces in

order to avoid recognition by cells of the mononuclear phagocyte system [20]. Schematic diagram of the experimental setup is shown in Fig. 2. Feeding rates were controlled by a micro feeder. Ultrasound irradiation was started at the time of the beginning of the addition of  $\text{FeSO}_4 \cdot 7\text{H}_2\text{O}$  aqueous solution using a multiwave ultrasonic generator (KAIJO, TA-4021, 200kHz, 6 W/cm<sup>2</sup>) connected with a PZT oscillator. Sonication was carried out under air, argon, nitrogen and oxygen. During the sonication, reaction vessel was cooled in the water bath (20°C). Preparation conditions are summarized in Table 1. In all experiments, irradiation time of ultrasound was 30min. The final concentrations of  $\text{FeSO}_4 \cdot 7\text{H}_2\text{O}$ , NaOH and PEG-MS at the end of the addition of  $\text{FeSO}_4 \cdot 7\text{H}_2\text{O}$  were 0.04 M, 0.08 M and 0.4 mM, respectively, and the total volumes were 50 ml. After ultrasound irradiation, products were collected by a neodymium magnet and rinsed with distilled water twice and dried in vacuo.

The crystallographic information of the products was obtained by XRD measurement (RIGAKU RINT-2200,  $\text{CuK}\alpha_1$ ,  $\lambda = 0.15418$  nm). The morphologies were observed by TEM (JEOL, JEM-2010-UHR, operated at 200kV), and the specimens for the TEM observation were prepared by the dispersion containing products was dropped on collodion film covered copper grid followed by drying under vacuum. The magnetic properties were evaluated by a superconducting quantum interference device (SQUID)(Quantum Design).

Sonochemically produced oxidants such as hydrogen peroxide, nitrite and nitrate ions were determined by colorimetric analyses. Hydrogen peroxide was determined by KI method [21]. Iodide ion is oxidized by  $\text{H}_2\text{O}_2$  in neutral or slightly acidic solutions and the absorption of iodine molecule is measured at 352 nm using a UV-vis spectrophotometer (Shimadzu UV-2100). The iodide reagent was prepared

immediately before use by mixing equal volumes (1.25 mL) of solution A (0.4 M KI, 0.05 M NaOH,  $1.6 \times 10^{-4}$  M  $(\text{NH}_4)_6\text{Mo}_7\text{O}_{24} \cdot 4\text{H}_2\text{O}$ ) and solution B (0.1 M  $\text{KHC}_8\text{H}_4\text{O}_4$ ). The sonicated sample solution (2 mL) was added to the solution described above and diluted with water to 5 mL.

In the determination of nitrite ions, nitrite ion reacts with primary amine to form diazonium salt, and then produce azo color compound via coupling reaction [22]. Typically, a 1 ml of sonicated sample solution containing nitrite ions was diluted to 10 ml with pure water. A 1ml of sulfanilic acid solution (1 g of sulfanilic acid was dissolved in 100 ml of 1% HCl) was added and kept for 15 min. Then, 1ml of 1% N-1-naphthyl ethylenediamine dihydrochloride solution was added and stood for 20 min. The absorbance of azo color compound at 546 nm was measured by using UV spectrometer.

In the cases of nitrate ions, nitro compounds derivated from nitrate ions were determined by a colorimetric method [23]. 1 ml of sonicated sample solution containing nitrate ions was mixed with 1ml of sodium salicylate (1 g of sodium salicylate was dissolved in 0.01 N NaOH) and 0.2% of sodium chloride and 0.1% of ammonium sulfamete solution, and kept in an oven (110°C) to be evaporated to dryness. Then, 2 ml of concentrated sulfuric acid was added and kept for 10min. 10 ml of pure water and 40% NaOH aqueous solution were added and distilled to 25 ml with pure water. Absorbance of nitro compounds at 412 nm was measured by using UV spectrometer.

### **3. Results and discussions**

Under the sonication, the color of the solutions of  $\text{Fe}(\text{OH})_2$  formed by the addition of  $\text{FeSO}_4 \cdot 7\text{H}_2\text{O}$  turned into dark brown, suggesting the formation of iron oxide



consisting of mainly magnetite. After the sonication, all products were readily collected by a magnet. In the absence of sonication, the greenish color of the sample suspension is formed, indicating that the iron hydroxide was not oxidized with 30 min of mechanical stirring. In the XRD measurements, all detected peaks can be assigned to the reflections from magnetite (the detailed results of XRD measurements will be mentioned later). TEM image and size distribution of the formed magnetite are displayed in Fig. 3. In the case of the constant feeding rate (= 5 ml/min), the sizes of magnetite nanoparticles decreased with the decreasing of the concentration of  $\text{FeSO}_4 \cdot 7\text{H}_2\text{O}$ . In the constant concentration (= 0.067 mol/l) of  $\text{FeSO}_4 \cdot 7\text{H}_2\text{O}$ , slower feeding rate lead to smaller and more uniform magnetite. Magnetite nanoparticles obtained by RHP method are found to be smaller than those made by NP method.

In order to investigate the effects of the sonication to the morphologies of the products, the addition of  $\text{FeSO}_4 \cdot 7\text{H}_2\text{O}$  aqueous solution (0.067 M, feeding rate of 1 ml/min) was followed by the sonication. TEM image and size distribution of the obtained magnetite nanoparticles are shown in Fig. 4, which show their size to be larger than those of RHP method. In general, magnetite nanoparticles are prepared by the oxidation of the solution of iron hydroxide obtained by the adding NaOH aqueous solution into an aqueous solution of iron salts. However, in RHP method, since an aqueous solution of  $\text{FeSO}_4 \cdot 7\text{H}_2\text{O}$  solution was slowly fed into NaOH aqueous solution, rapid and localized changes of pH value in the sample solution were restricted. Furthermore, formed iron hydroxide were dispersed into small particles and effectively oxidized due to ultrasound irradiation. These results suggest that the morphologies of the finally formed oxides depended on the timing of sonication, probably on the dispersities of the intermediate metal hydroxides  $\text{Fe}(\text{OH})_2$ .

Fig.5 shows magnetization curves of the obtained magnetite nanoparticles prepared at the constant concentration of  $\text{FeSO}_4 \cdot 7\text{H}_2\text{O}$  (0.067 M). Saturation magnetization became small with the decreasing of feeding rate of  $\text{FeSO}_4 \cdot 7\text{H}_2\text{O}$ , because their particle sizes also became small with the decreasing of feeding rate. The saturation magnetization of the product prepared by 5 mL/min of feeding rate was 70.2 emu/g under  $5 \times 10^4$  Oe at room temperature (300 K). Additionally, in the all magnetization curves, residual magnetization and coercivity are almost zero at room temperature. So, it was recognized that the obtained magnetite nanoparticles are magnetically soft. The changes in zero-field cooled (ZFC) and field cooled (FC) magnetization under 100 Oe of external magnetic field are shown in Fig.6. The ZFC magnetization at lower temperature was much lower than the FC magnetization. Under ZFC condition, the magnetite nanoparticles became magnetically frozen and their magnetic moment could not align along the direction of the external magnetic field. The spins became able to rotate about 200 K at which the maximum value of magnetization was obtained and the ZFC magnetization curve nearly overlapped the FC curve. The magnetite nanoparticles by RHP method display superparamagnetic property above about 200 K.

Fig.7 shows XRD patterns of the product under air, oxygen, nitrogen, and argon. XRD patterns of the product without sonication and commercially available magnetite (purchased from Kojundo Kagaku, ca. 1 $\mu\text{m}$ -diameter) are also displayed. In the pattern of the product under air, the peaks reflected from magnetite are sharp and high in intensity. In contrast, in the patterns of the products under other gases and the product without sonication, the peaks from magnetite are broad and ambiguous, suggesting lower yield together with the low crystallinity or amorphous structure. The

facts indicate that the progress of the oxidation and crystallization of magnetite depend on the sonication atmosphere. The formation process of magnetite include i) oxidation of Fe(II), ii) Fe(II) adsorption on the surface of Fe(III) oxides, and iii) crystallization of magnetite [24, 25]. The formation of magnetite depend on the oxidation rate of green rust, which is formed between ii) and iii) [26].

To investigate the effects of sonication atmospheres, the oxidants produced in various gases saturated-neutral waters were determined. Fig.8 shows oxidants yields produced by sonicating 50 ml of water for 30 min under air, oxygen, nitrogen, and argon atmospheres. In the presence of air, hydrogen peroxide, nitrite and nitrate ions were produced and total amounts of the produced oxidants were largest among the investigated gases. Only hydrogen peroxide was produced under oxygen or argon. In the case of nitrogen, hydrogen peroxide, nitrite and nitrate ions were detected but the amounts quite small.

In the sonochemical reactions in aqueous solution, water molecules are thermally decomposed to form hydrogen atom ( $\cdot\text{H}$ ) and hydroxyl radical ( $\cdot\text{OH}$ ), which of them are recombined to form hydrogen, hydrogen peroxide, and parent water [19]. Under atmosphere including oxygen, which is a good scavenger of hydrogen atom [27], recombination between hydrogen atoms and hydroxyl radicals is prevented. Accordingly, higher amounts of hydrogen peroxide would be obtained when oxygen or air dissolved in water. Sonochemical formation of nitrite and nitrate ions in aerated water has been well known [28-30] and the following pathway was proposed [31].



As shown, for the formations of nitrite and nitrate ions, both of nitrogen and oxygen are required. In the case of sonication under air, nitrite and nitrate ions were formed, however, under nitrogen those yields were little. Tada et. al. reported preparation of magnetite nanoparticles using hydrogen peroxide as oxidant[32]. The contribution of nitrate ions to the oxidation of  $Fe(OH)_2$  to form magnetite was reported separately [33]. According to the oxidants yields and XRD patterns, it is considered that hydrogen peroxide, nitrite and nitrate ions act as oxidants in sonochemical formation of magnetite nanoparticles.

## Conclusions

We demonstrated the sonochemical preparations of magnetite nanoparticles by RHP method. In RHP, the feeding conditions of  $FeSO_4 \cdot 7H_2O$  solution such as feeding rates and the timing of sonication had important effects on the sizes and their distributions, namely slower feeding rate and lower concentration lead to smaller and more uniform shaped magnetite nanoparticles. Furthermore, the timings of ultrasound irradiation were also significant to prepare smaller and more uniform-shaped magnetite, i.e. simultaneous sonication with  $FeSO_4 \cdot 7H_2O$  aqueous solution feeding is required. The obtained magnetite nanoparticles had about 10 nm in average diameter and exhibited superparamagnetism of which characters are favorable in the application

in nanobiotechnologies.

The mechanisms of sonochemical oxidation were also discussed. Oxidizing conditions of the products varied with the dissolved gases. The results of the quantitative analyses of sonochemically produced oxidants showed hydrogen peroxide, nitrite and nitrate ions acted as oxidants. Since the highest yields of the oxidants were obtained under air, it was concluded that both oxygen and nitrogen were necessary for the effective sonochemical oxidation.

### **Acknowledgements**

This study was partially supported by Iketani Science and Technology Foundation. The authors thank Dr. Takuya Kinoshita (Osaka Prefecture University), Dr. Satoshi Seino and Prof. Takao A. Yamamoto (Osaka University) for their helpful assistance in the evaluation of magnetic properties.

## References

1. N. Spaldin, *Magnetic Materials: Fundamentals and Device Applications*, Cambridge University Press: Cambridge, 2003.
2. S. Chikazumi, S. Taketomi, M. Ukita, K. Mizukami, H. Miyajima, M. Setogawa, Y. Kurihara, *J. Magn. Magn. Mater.* 65 (1987) 245.
3. R. Y. Hong, T. T. Pan, H. Z. Li, *J. Magn. Magn. Mater.* 303 (2006) 60.
4. A.-H. Lu, W. Schmidt, N. Matossevitch, H. Bönnermann, B. Tesche, E. Bill, W. Kiefer, F. Schüth, *Angew. Chem. Int. Ed.* 43 (2004) 4303.
5. Y. Mizukoshi, K. Sato, T. J. Konno, N. Masahashi, S. Tanabe, *Chem. Lett.* 37 (2008) 922.
6. T. Heyon, *Chem. Commun.* (2003) 927.
7. D. W. Elliot, W.-X. Zhang, *Environ. Sci. Technol.* 35 (2001) 4922.
8. M. Takafuji, S. Ide, H. Ihara, Z. Xu, *Chem. Mater.* 16 (2004) 1977.
9. H. Gu, K. Xu, C. Xu, B. Xu, *Chem. Commun.* (2006) 941.
10. (a) T. Kinoshita, S. Seino, Y. Mizukoshi, T. Nakagawa, T. A. Yamamoto, *J. Mag. Mag. Mater.* 311 (2007) 255; (b) Y. Mizukoshi, S. Seino, T. Kinoshita, T. Nakagawa, T. A. Yamamoto, S. Tanabe, *Scripta Mater.* 54 (2006) 609; (c) Y. Mizukoshi, S. Seino, K. Okitsu, T. Kinoshita, Y. Otome, T. Nakagawa, T. A. Yamamoto, *Ultrason. Sonochem.* 12 (2005) 191.
11. H. Gu, P.-L. Ho, K. W. T. Tsang, L. Wang, B. Xu, *J. Am. Chem. Soc.* 125 (2003) 15702.
12. J. Sudimack B. A., R. J. Lee, *Adv. Drug Delivery Rev.* 41 (2000) 147.
13. R. Weissleder, A. Bogdanov, E. A. Neuwelt, M. Papisov, *Adv. Drug Delivery Rev.* 16 (1995) 321.

14. O. S. Nielsen, M. Horsman, J. Overgaard, *Eur. J. Cancer* 37 (2001) 1587.
15. A.-H. Lu, E. L. Salabas, F. Schüth, *Angew. Chem. Int. Ed.* 46 (2007) 1222.
16. H. Yang, Y. Xia, *Adv. Mater.* 19 (2007) 33.
17. T. Shuto, Y. Mizukoshi, S. Tanabe, H. Kurokawa, *IEICE Transactions on Fundamentals of Electronics, Communication and Computer Sciences* J89-A (2006) 729.
18. Y. Teraoka, S. Nanri, I. Moriguchi, S. Kagawa, K. Shimano, N. Yamazoe, *Chem. Lett.* 29 (2000) 1202.
19. For example, T. J. Mason (Ed.), *Advances in Sonochemistry* Vol.1, JAI Press: London, 1990.
20. R. Gref, M. Lück, P. Quellec, M. Marchand, E. Dellacherie, S. Harnish, T. Blunk, R. H. Müller, *Colloid Surf B- Biointerf.* 18 (2000) 301.
21. A. E. Alegria, Y. Lion, T. Kondo, P. Riesz, *J. Phys. Chem.* 93 (1989) 4908.
22. S. Teramoto, R. Saito, Y. Shirasu, *Teratology* 21 (1950) 71.
23. (a) J. L. Lambert, F. Zitomer, *Anal. Chem.* 32 (1960) 1684; (b) Kanno, S. Fukui, M. Kaneko, *Eiseikagaku* (Japanese journal of toxicology and environmental health) 14 (1968) 24.
24. T. Misawa, K. Hashimoto, S. Shimodaira, *Corrosion Sci.* 14(1974) 131.
25. Y. Tamaura, P. V. Buduan, T. Katsura, *J. Chem. Soc. Dalton Trans.* 9 (1981) 1807.
26. J.-M. R. Génin, A. A. Olowe, P. H. Rafait, L. Shimon, *Corrosion Sci.* 38 (1996) 1751.
27. A. Henglein, *Naturwissenschaften* 43 (1956) 277.
28. A. I. Virtanen, N. Ellfork, *J. Am. Chem. Soc.* 72 (1950) 1046.
29. A. Henlein, M. Gutierrez, *Int. J. Radiat. Biol.* 50 (1986) 527.
30. Supeno, P. Kruus, *Ultrason. Sonochem.* 7 (2000) 109.

31. E. L. Mead, R. G. Sutherland, R. E. Verrall, *Can. J. Chem.* 54 (1976) 1114.
32. M. Tada, S. Hatanaka, H. Sanbonsugi, N. Matsushita, M. Abe, *J. Appl. Phys.* 93 (2003) 7566.
33. T. Sugimoto, E. Matijević, *J. Colloid. Interf. Sci.* 74 (1980) 227.



## Figure Captions

Fig. 1 TEM image and size distribution of magnetite nanoparticles prepared by normal precipitation method.

Fig. 2 Schematic diagram of the reaction setup.

Fig. 3 TEM images and size distributions of magnetite nanoparticles prepared at the conditions of (run a) 0.2 M, 5 ml/min ;(run b) 0.1 M, 5ml/min ;(run c) 0.067 M, 5ml/min ;(run d) 0.067 M, 3ml/min;(run e) 0.067 M 1ml/min.

Fig. 4 TEM images and size distribution of magnetite nanoparticles sonicated after the addition of  $\text{FeSO}_4 \cdot 7\text{H}_2\text{O}$  aqueous solution.

Fig. 5 Magnetization curves of magnetite nanoparticles prepared at the feeding rates of 5ml/min (run c), 3ml/min (run d), and 1ml/min (run e).

Fig. 6 Zero field cooled (ZFC) and field cooled (FC) magnetization curve as a function of temperature (applied field = 100 Oe) for the magnetite nanoparticles (run e).

Fig. 7 XRD patterns of (1)purchased and sonochemically prepared maghemite under (2) air, (3) oxygen, (4) argon, (5) nitrogen, (6) without sonication.

Fig. 8 Oxidants yields in neutral waters sonicated under various atmospheres.

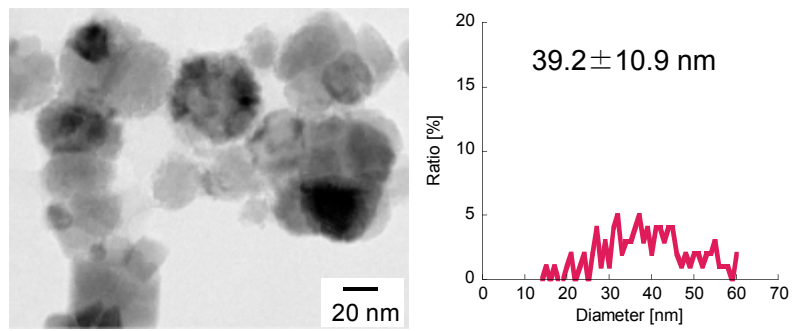


Fig. 1

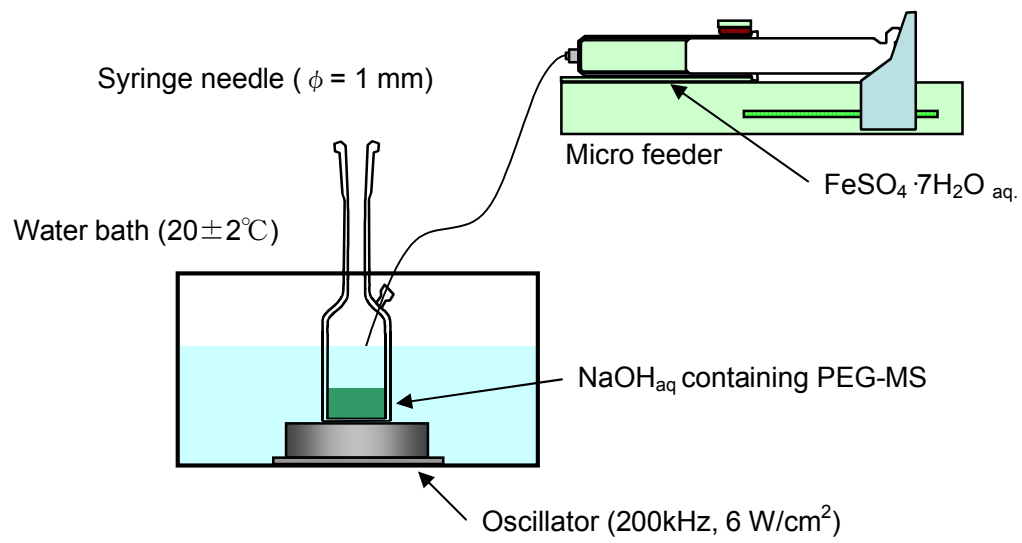


Fig. 2

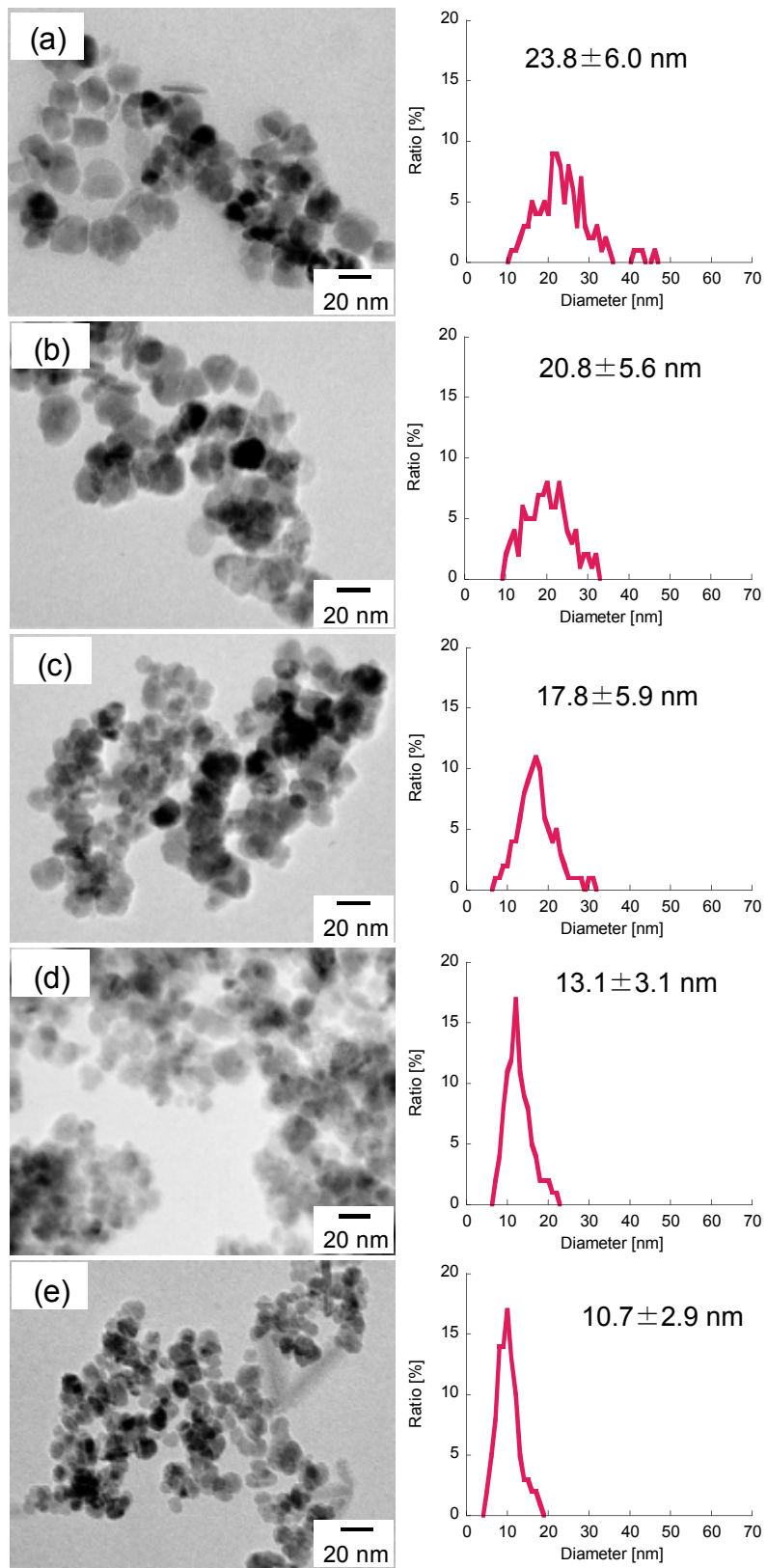


Fig.3

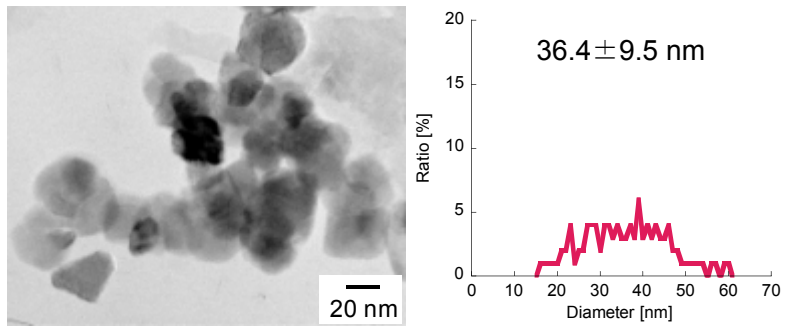
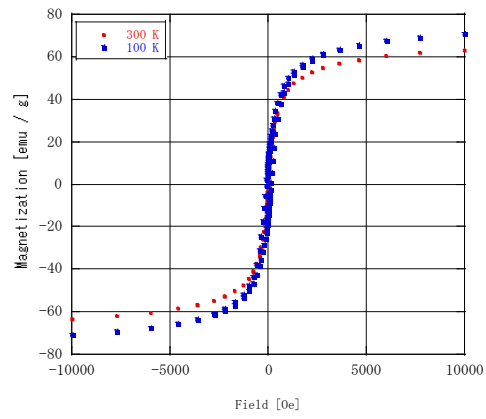
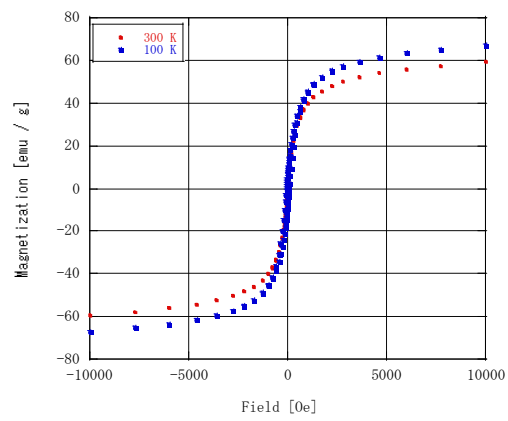


Fig. 4

(run c)



(run d)



(run e)

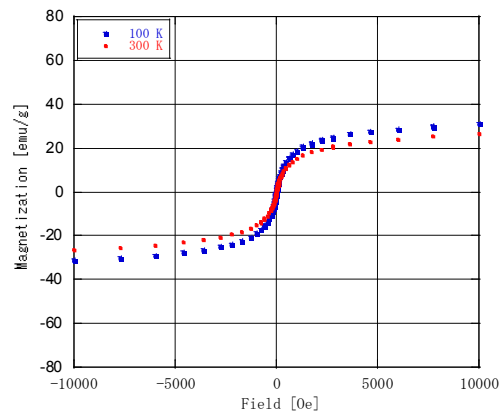


Fig. 5

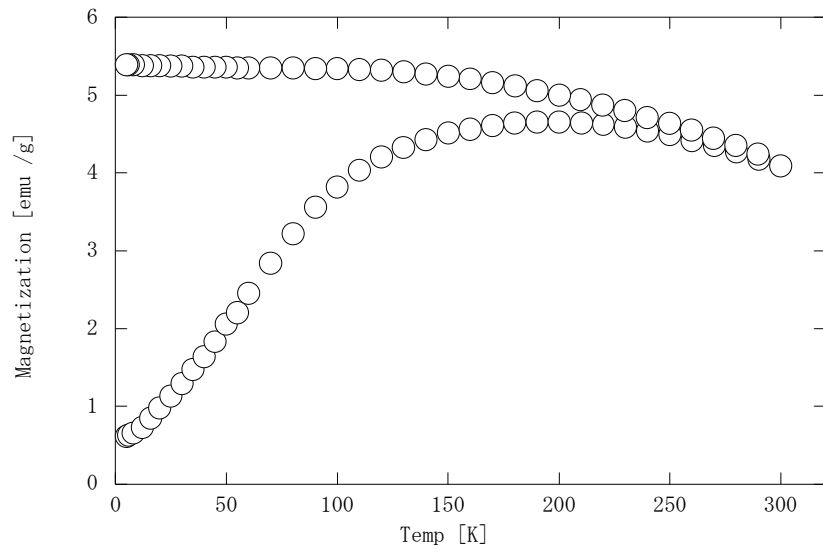


Fig.6

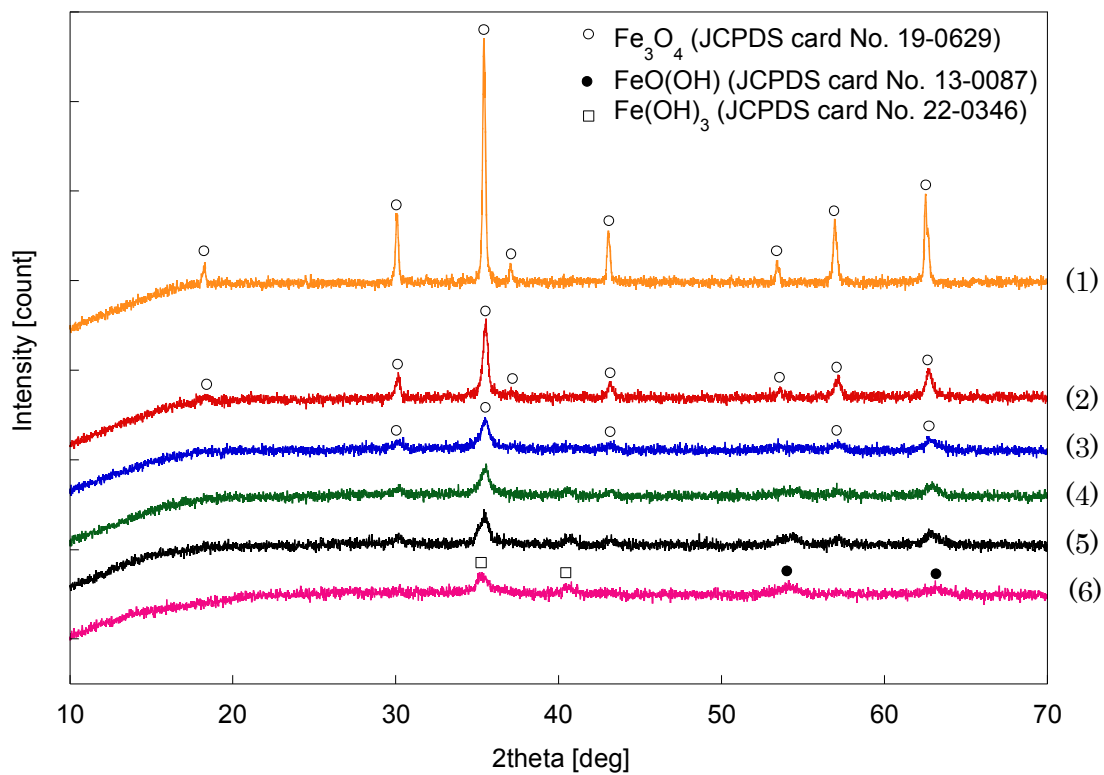


Fig.7

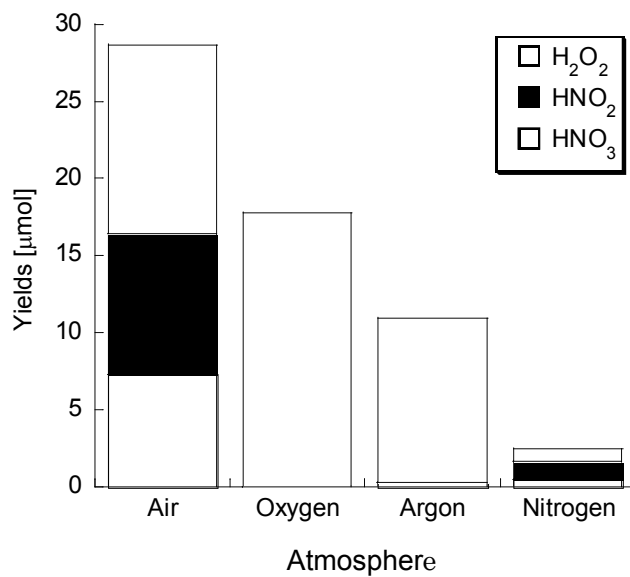


Fig. 8

**Table 1 Preparation conditions of reverse precipitation method.**

Run	FeSO <sub>4</sub> ·7H <sub>2</sub> O				NaOH				Total Volume / ml
	Amounts / mmol	Volumes / ml	Concentration / mol·l <sup>-1</sup>	Feeding rates / ml·min <sup>-1</sup>	Amounts / mmol	Volumes / ml	Concentration / mol·l <sup>-1</sup>	Amounts of PEG-MS / mmol	
a	2	10	0.2	5	4	40	0.1	0.02	50
b	2	20	0.1	5	4	30	0.133	0.02	50
c	2	30	0.067	5	4	20	0.2	0.02	50
d	2	30	0.067	3	4	20	0.2	0.02	50
e	2	30	0.067	1	4	20	0.2	0.02	50